ISSN 2063-5346

Section A-Research paper

Investigation of Compaction Pressure on PolylactidAcid/Polycaprolactone/Nano Hydroxyapatite Composite Materials Prepared by Cold Isostatic Pressing Method

Solechan[1,2*]
[1]Department of Mechanical Engineering, Faculty of Engineering, Diponegoro University, Semarang 50275, Indonesia.
[2]Department of Mechanical Engineering, Universitas Muhammadiyah Semarang, Kampus Kasipah, Semarang 50254, Indonesia.
Agus Suprihanto[1]
[1]Department of Mechanical Engineering, Faculty of Engineering, Diponegoro University, Semarang 50275, Indonesia.
Susilo Adi Widyanto[1]
[1]Department of Mechanical Engineering, Faculty of Engineering, Diponegoro University, Semarang 50275, Indonesia.
Joko Triyono[3]
[3]Department of Mechanical Engineering, Sebelas Maret University, Surakarta 57126, Indonesia
***Corresponding Author:** solechan@unimus.ac.id

ABSTRACT

Most patients with fracture injuries due to accidents are the femur. Internal fixation of plates and screws as a medium for healing femoral fractures. Internal fixation of plates from PLA/PCL biodegradable polymers is the most widely used to replace metals. Biodegradable polymers have many weaknesses in terms of mechanical strength which is still low and the rate of degradation is difficult to control. The addition of nHA reinforcement to form composite materials with the cold isostatic pressing method at high compaction pressure can increase mechanical strength. PLA/PCL/nHA composite materials were made into specimens for characters that can reduce the porosity's size and increase mechanical strength. High compaction pressure has no significant effect on material properties. The proof is that the FTIR test of the three specimens still has band peaks which are identified as elements of the PLA/PCL/nHA composite material. The XRD test results prove the same, which show a widened diffraction peak. This means that there are no crystal peaks in the composite material, this proves that the structure is amorphous, the level of crystallinity is low and the degradation time is faster. The most optimal compressive and tensile strength test results at a compacting pressure of 40 MPa with a compressive strength value of 71.2 N and a tensile strength of 23.36 N/mm2. This compaction pressure can reduce the porosity's size, the surface is smoother, the interfacial bonds are stronger, the density is high and the mechanical strength increases larger. However, the compressive and tensile strength is still below the strength of the femur bone at the implant site.

Keywords : Composite, Femur, Plate, Isostatic, Polylactic Acid, Hydroxyapatite

1.0 Introduction

Fractures due to traffic accidents are most common in the femur. Fractures can cause bleeding, internal organ injuries, wound infections, and disability [1]. Healing of femoral fractures uses the internal fixation of plates and screws that are placed on cracked or broken parts [2]. The installation is designed to support and support body weight until the bone remodeling or bones heal [3]. Many plates internal fixations are made of metal materials, such as cobalt, stainless steel, titanium, metal alloys, and composites [4,5]. The advantages of metal materials are biological adaptation, biocompatible, corrosion resistance, rigidity, and good mechanical strength [6]. Deficiency can in infection, discomfort, inflammation, traumatic patient,

ISSN 2063-5346

risk of surgical complications, allergic reactions, stress shielding, two surgical operations, and high treatment costs [7-9].

Evaluation of the lack of internal fixation of metal plates, now the use of biodegradable and biocompatible polymer materials is more developed and researched [10-12]. Internal fixation of plates from biodegradable polymers has many advantages, including no post-healing bone removal, degradation in the body, comfort, painlessness, and reduced operating costs [13,14]. Meanwhile, the drawbacks are low mechanical strength, difficulty to mix, low adhesion, and the rate of degradation is difficult to control [15,16]. Polylactic Acid (PLA) and Polycaprolactone (PCL) as biodegradable polymers are often used in the manufacture of plate internal fixation [17,18]. PLA and PCL have gradual degradation properties, the rate of degradation can be controlled, high impact toughness, and able to transfer loads from the supporting structures of the body when the bone has been remodeled [19-21]. PCL mixed with PLA can increase the ductility and toughness of the internal fixation of the plate. PLA is better than PCL in terms of cell adhesion and proliferation due to its hydrophilic nature, while PCL has hydrophobic properties and is not physiologically active so cell growth does not occur when in contact with biological cells [22,23].

Ferri. J et al. (2016) conducted a mixture of PLA/PCL materials for a mixture ratio of 70/30 to have optimal results [24]. The highest elastic modulus, increased impact strength, and small crack development, but the strength are still below the buckling strength of the femur of 130 MPa [25]. Fortelny et al. (2019) made an internal plate fixation of PLA/PCL with the most optimal composition of 80/20. The result is that the toughness is quite high, the tensile strength increases by 20%, and the stiffness decreases, but the tensile strength is still below that of the femur [26]. Mechanical strength is still low, so it is necessary to increase its strength by adding reinforcing materials to form composite materials [15,16]. Nano hydroxyapatite (nHA) is a ceramic material that many researchers recommend as a reinforcing material for PLA/PCL blends [27,28]. The advantages of nHA are that it has biocompatible, osteoconductive, and noncytotoxic properties, is very hard, has a slow degradation rate and its crystal biology is similar to human bone. However, nHA has drawbacks including being difficult to mix, brittle, low elasticity, and limited application [29,30]. PLA/PCL/nHA is a composite material that can increase mechanical strength and control the rate of degradation [18,31].

Combining PLA/PCL/nHA composite materials to reinforce each other so that good mechanical strength is formed [32,33]. The addition of nHA made through the cold isostatic pressing method with variations in compacting pressure can increase density, reduce porosity, uniform density, increase hardness, reduce distortion, and smooth surfaces [34-37]. Fitriyana et al. (2022) examined the effect of using mixed HA on PLA/PCL (80/20 wt%) with variations in compaction pressure. As a result, the addition of HA improves the mechanical, physical properties, and the degradation can be controlled. However, the addition of HA is greater for faster degradation [38]. Balbinotti. P et al. (2011), made implants with HA/Ti composite materials using the hot isostatic pressing method. Compaction pressure 600 MPa, temperature 1200°C for 2 hours in an argon atmosphere. HA exhibits a more uniform agglomerate distribution and higher compressive strength [39].

Guangyao et al. (2016) performed the characterization of Hydroxyapatite/Magnesium (Hap/Mg) composite materials for biomedical implants using a powder compaction process. The composition of the HAp content is 5, 10, and 15%. The mixture was compacted at a pressure of 40 MPa with a hot isostatic pressing temperature of 500oC for 10 minutes. The addition of 15% HA can be uniformly distributed, high density, and increased compressive strength [40]. The manufacture of internal fixation of plates by hot isostatic pressing has been extensively studied, while cold isostatic pressing has not been studied intensively. This research wants to know the variation of powder compaction pressure using the cold isostatic pressing method in the manufacture of internal fixation plates with PLA/PCL/nHA composite materials. This material is expected to have the same characteristics and mechanical strength as the femur bone implanted with internal fixation plates.

2.0 MATERIALS & METHODOLOGY

Materials for making specimens for internal fixation of plates using PLA/PCL/nHA composite materials. PLA material in powder form with the chemical formula (C6H8O5)n, density 1.24 gr/cc, melting point 175-220℃ was made by Repreper Tech Co, Kowloon, Hongkong. PCL material obtained from Solve Interox Limited Wand arrington UK, in powder form with the chemical formula (C6H8O2)x, density 1.1 gr/cc and melting point 58-60℃. nHA material as a reinforcing material with a powder size of 500-100 nm with >99% purity. It is white in color, has a density of 3.076 gr/cm3, and a melting point of 1100℃. nHA is manufactured by Sigma-Aldrich Pte Ltd, Pasir Panjang, Singapore. The composition of the composite material for PLA/PCL/nHA tablet and stem specimens with a percentage of 80+20/20 wt% for the total weight is shown in Table 1.

Table 1. Specimen weight of PLA/PCL/nHA composite material composition

Specimen	PLA80 %wt (gr)	PCL20% wt (gr)	nHA20% wt (gr)	Total Weight (gr)
Tablet	0,96	0,24	0,3	1,5
Stem	12,8	3,2	4	20

Preparation of specimens from PLA/PCL/nHA composite materials using the cold isostatic pressing method of powder compaction. First the process of weighing the PLA/PCL/nHA material using an analytical balance with an accuracy of 0.0001g. The second is mixing PLA/PCL/nHA material with ball milling brand Bexco made by Haryana, India at 80 rpm for 2 hours. Furthermore, the compaction process using the cold isostatic pressing method at a temperature of 30^{o}C with a pressure variation of 30, 35, 40 MPa. Taking the green body from the mold, then sintering it with a temperature of 150℃ in an industrial digital oven type D1570 made in Taiwan. The holding time for 2 hours in the digital oven. The finish process is testing the specimen with Fourier Transform Infrared Spectroscopy (FTIR), Scanning Electron Microscope (SEM), density, porosity, bending, and tensile tests.

3.0 Results and Discussion

3.1. Fourier Transform Infrared Spectroscopy

FTIR test results with detected spectrum pattern at 2921.29 cm^{-1} and 2853.33 cm^{-1} with wide bands for C–H stretch elements in PCL are shown in Figure 1. This indicates that the peaks are in the region of the stretching band according to the PCL material detected as CH_2 [41]. PLA was detected at the peak of the spectrum of 1715.31 cm^{-1} according to the C=O stretch bond included in the carboxylic acids group. The PCL spectrum which has C–O ester bonds in the range 1300-1000 cm^{-1} it is detected from a peak of 1152.49 cm^{-1} and this represents the spectrum in the PLA/PCL blends [12,42,43]. PLA is inert so it does not have a group chain with a reactive side [44]. Absorption bands (v_3PO4^{-3}) of nHA were identified around 1030 cm^{-1} and 1090 cm^{-1}.

These results are in accordance with the research of Dahlan et al. (2006) for HA identified around 1042.54 cm^{-1}. Analysis of the spectrum of phosphate crystallinity can evaluate the absorption of phosphate $v_4$4PO4^{-3}. Calcium phosphate can be characterized by the presence of the absorption band v_4 in the form of a maximal cleavage with the presence of bands at 564 cm^{-1} and 602 cm^{-1} [45]. These results prove the similarity of the maximum spectrum peaks at 562.60 cm-1 and 601.73 cm^{-1}. The presence of identified band peaks indicates the presence of peaks from the PLA/PCL/nHA composite material. the findings in the composite material caused the PLA surface to be unable to bond chemically with the nHA powder surface. These results were concluded because the PLA/PCL blends, and nHA did not form chemical bonds, this was because PLA had hydrophobic properties [46].

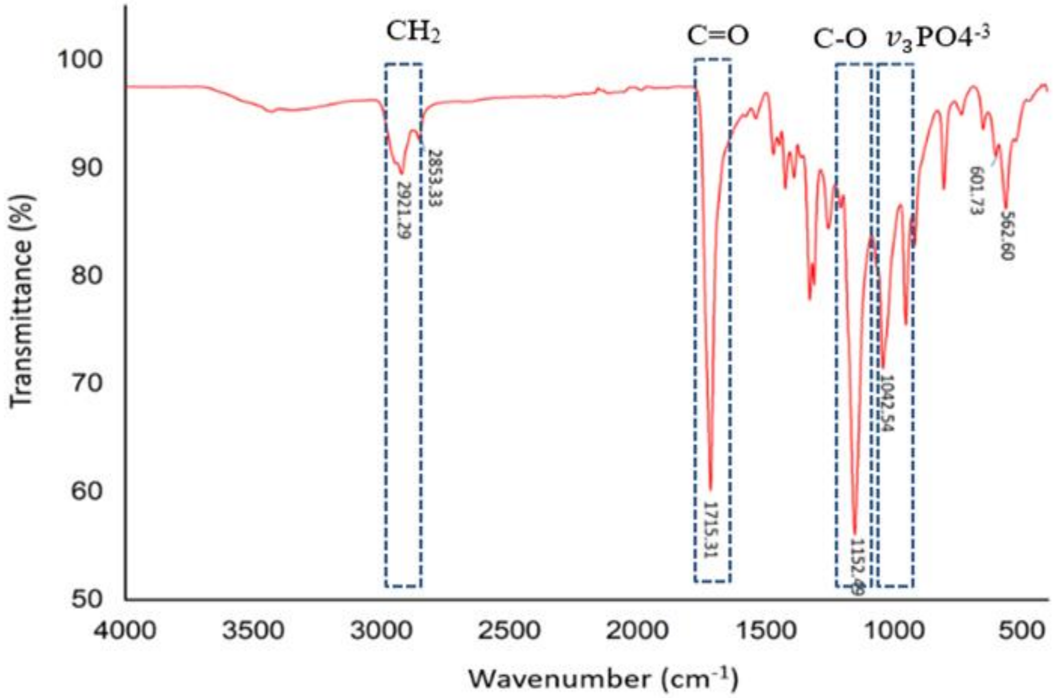

Figure 1. FTIR spectrum on PLA/PCL/nHA composite materials

3.2. X-Ray Diffraction

PLA/PCL/nHA composite material specimens with various compaction pressures of 30, 35, and 40 MPa were subjected to the XRD test. This test examines the change in patch crystallinity of the diffraction peaks in the measurement range of 5 to 90^{o} (2θ). The results of the XRD test with variations in pressure are shown in Figure 2 to see the crystal form, structure, and elements in the specimen. Compaction pressure at 30, 35, and 40 MPa showed peaks of 2θ= 23.58^{o}, 22.51^{o}, and 22.26^{o} at the same intensity level. The three peaks formed belong to the PLA/PCL blends [12]. While nHA is formed at the peak of 2θ = 26^{o}. This indicates that the PLA/PCL/nHA composite material only shows a broad peak positioned between 10^{o} and 40^{o}. The absence of sharp crystalline peaks in the PLA/PCL/nHA composite material indicates that the structure formed is amorphous [47]. In accordance with the research conducted by Hou et al. (2019) for the XRD graphic pattern of the PLA/PCL blends with overlapping crystal peaks of the PCL phase in the amorphous PLA phase [48].

PLA is amorphous in PLA/PCL blends, which is characterized by non-sharp peaks with low absorption intensity. This is due to the difference in the degree of deformation of the PLA and PCL molecules during the specimen-making process. This proves that the PLA/PCL/nHA composite material has a low level of crystallinity which can shorten the degradation time or high degradation rate [46,49]. The presence of nHA causes a less uniform structure and regular crystallization, the distance between the PLA layers increases, which indicates an amorphous phase [50]. The presence of a low crystalline phase in all composite material specimens indicated the presence of 20%, which inhibited crystallization in the

ISSN 2063-5346

polymer matrix. The intensity of the PLA and PCL diffraction peaks did not increase with HA content. instead, everything got smaller and wider. The presence of nHA disrupts the molecular arrangement of PLA and PCL, thereby preventing crystal formation. this has no effect on variations in powder compaction pressure [51].

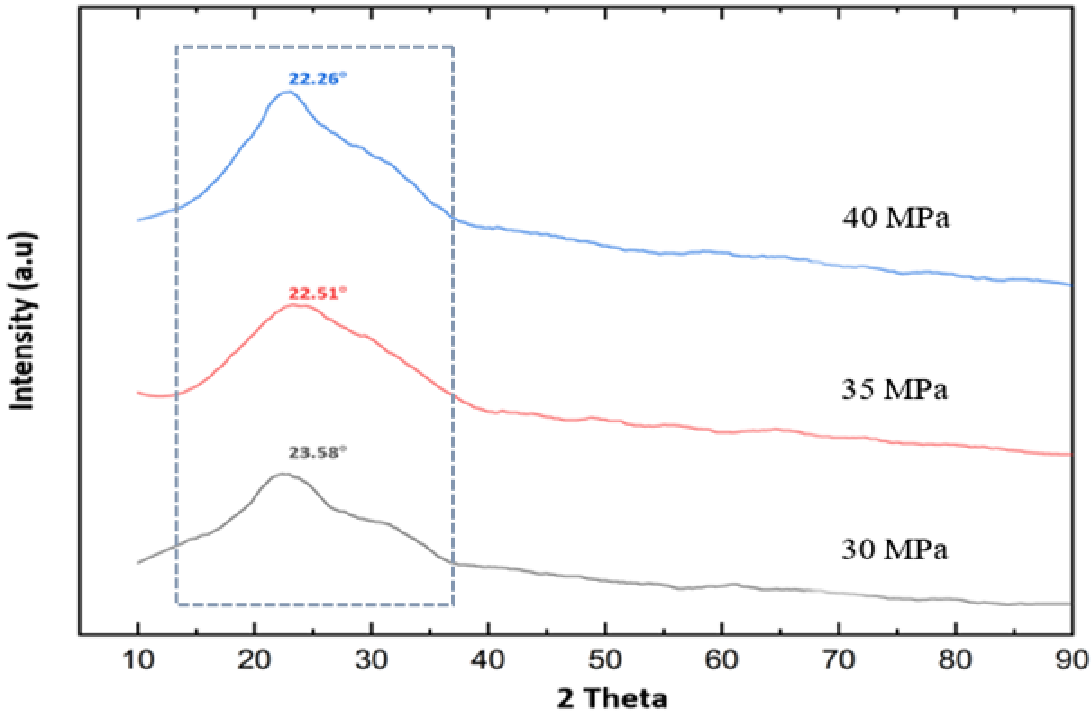

Figure 2. XRD diffraction graph of PLA/PCL/nHA composite material

3.3. Scanning Electron Microscope (SEM)

SEM photos of tablet specimens on PLA/PCL/nHA composite materials with various compaction pressures of 30, 35, and 40 MPa are shown in Figure 3. The SEM photo of the specimen at a compaction pressure of 30 MPa in Figure 4a shows white granular nHA evenly distributed over the entire surface. nHA and PCL are on the surface of PLA. PCL is in the form of a white agglomerate, while PLA is black. Low compaction pressure results in high porosity, large pores, and nHA only adhering to the surface. The surface bond between PLA and PCL is not very strong because little is mixed and it reduces the material interface contact. This finding is in line with research conducted by Gong. M et al. (2017). Increasing the compaction pressure to 35 MPa can increase the surface energy and interfacial contact between the PLA/PCL blends and nHA as shown in Figure 4b [52]. Besides that, it is able to reduce the agglomeration of nHA particles with a polymer matrix [41,53]. The porosity value is smaller, the pore holes are shallow, and not as abundant as at a compaction pressure of 30 MPa. Figure 4c from the SEM photo shows very little porosity, small pore holes, smoother surface, and high density due to the increased compaction pressure to 40 MPa.

The high compaction pressure in the cold isostatic pressing method can expand the material interface contact. This accelerates diffusion to form stronger interfacial bonds that occur in the sintering process [36]. The PLA/PCL blends are uniformly distributed and thoroughly mixed making porosity reduced which can add to high tensile and compressive strength [39,40].

The high compacting pressure was unable to adhere the nHA into the PLA/PCL blends and only stuck to the surface of the material, resulting in low interfacial bond strength. The nHA particles do not stick together in the polymer matrix due to dispersion problems that occur during the mixing process of the raw materials. A mixture of nHA particles with PLA/PCL needs to be added with a coupling agent or chloroform to increase the wettability of the particles which can reduce agglomeration and produce a homogeneous dispersion of nHA particles [29,54].

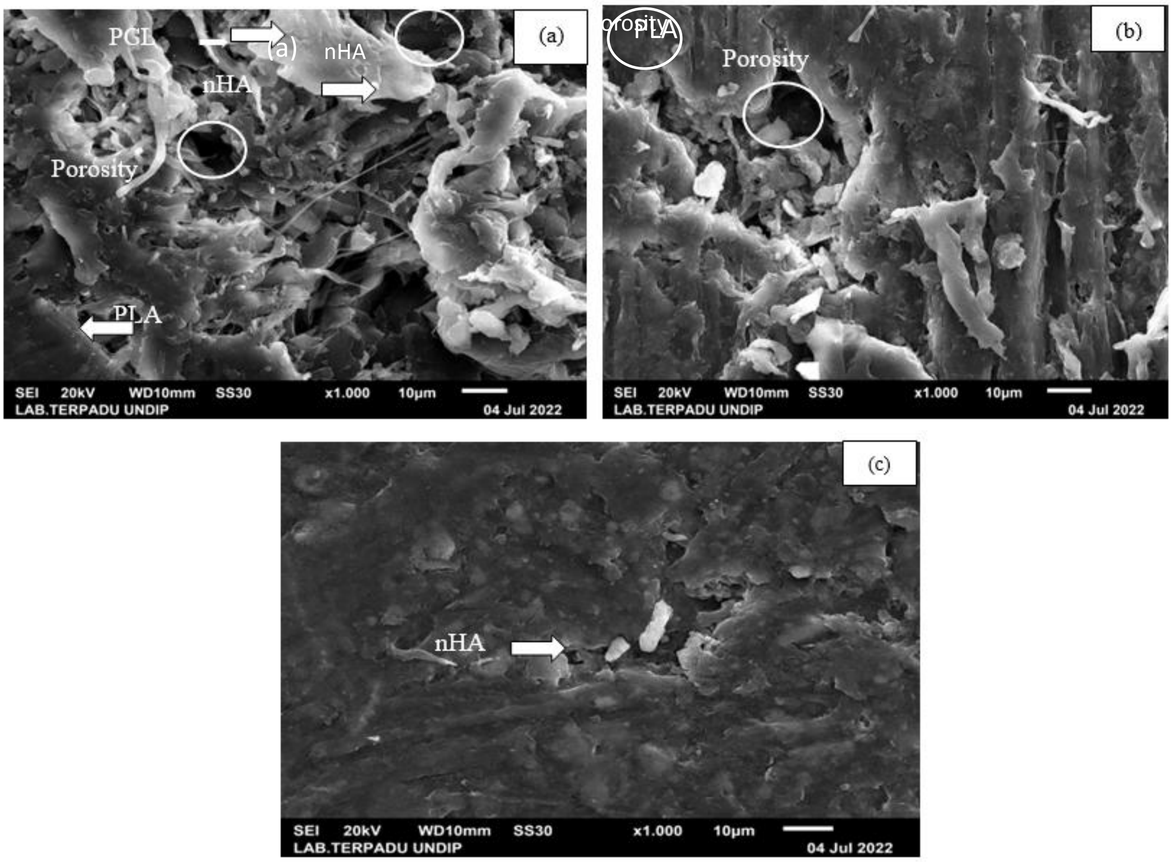

Figure 3. SEM photo of the specimen on the composite material at compaction pressure a). 30, b). 35, and c). 40 MPa

3.4. Density dan Porosity

Density and porosity testing used a densitometer scale MH-300A which was carried out in 2 stages. The first stage of the actual test is weighing the specimen in dry and wet conditions. the second stage is calculating the theoretical density [55]. Actual and theoretical density values to find porosity in percentage units (%). Density and porosity tests have a correlation that influences each other. Table 2 shows the results of testing the density and porosity of the PLA/PCL/nHA composite material specimens with various compaction pressures. Calculating volume for tablet specimens is obtained from calculating dimensions, then proven by theoretical calculations of weight divided by density. The most optimal results of density and porosity measurements of composite materials at a compaction pressure of 40 MPa were 1.384 g/cm^3 and 1.32%. After the compaction pressure was lowered to 35 MPa, the density decreased by 3.14% and the porosity increased by 58%.

Table 2. Density and porosity for PLA/PCL/nHA composite materials

Specimen PLA/PCL/nHA	Dry Weight DW (g)	Wet Weight Ww (g)	Volume V (cm³)	Density Pt (g/cm³)	Density Pc (g/cm³)	Porosity (%)
30 MPa	1.34	0.33	1.01	1.326	1.370	3.27
35 MPa	1.41	0.35	1.06	1.330	1.358	2.09
40 MPa	1.26	0.35	0.91	1.384	1.402	1.32

Figure 4 shows the smallest density of 1.326 g/cm^3 (0.3% decrease) and the largest porosity of 3.27% (56% increase) at a compaction pressure of 30 MPa. Higher compaction pressure can increase density and reduce porosity in PLA/PCL/HA composite materials [56,57]. High compaction pressure results in a smaller pore size as evidenced by SEM photos by increasing the contact area of the powder particle interface which is getting bigger. This is in accordance with the findings of Molinero et al. (2018) [58]. Increasing the compaction pressure in the cold isostatic pressing method causes changes in the structure of the particles to bind together and the number of pores decreases, this can increase the mechanical strength [59,60]. mixing nHA into the polymer matrix makes the interfacial linkages wider, making the bond stronger and the surface roughness smoother [61,62]. The effect of presence of nHA also inhibits the sintering of matrix materials (PLA/PCL), resulting in a greater percentage of porosity in composite materials [63].

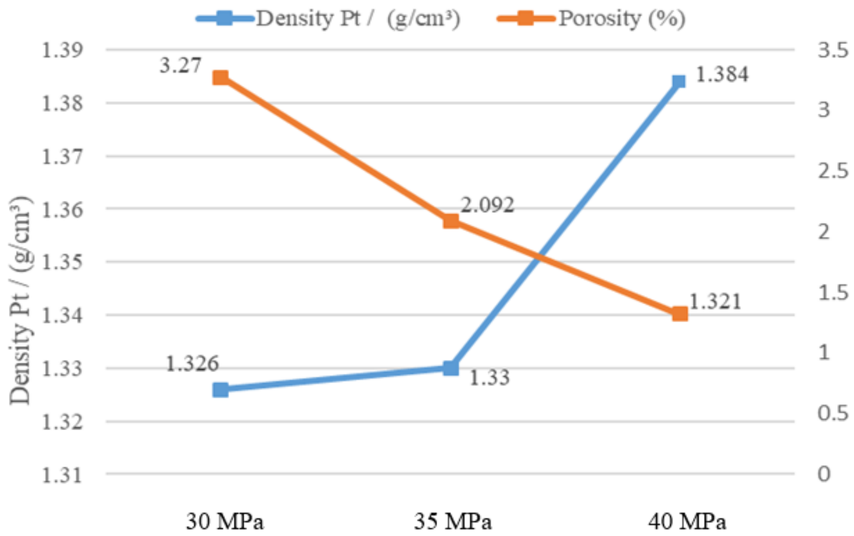

Figure 4. Density and porosity test results on composite materials

3.5. Bending Test

Specimens in composite materials with pressure variations in a three-point bending test to obtain the value of Max Force (N) and the amount of displacement (%) applied to the specimen until it breaks. Figure 5 shows a graph of the bending test results for PLA/PCL/nHA composite material specimens. The bending strength of the specimen received the highest load at a compaction pressure of 40 MPa of 71.2 N with a displacement of 6.1 mm. Specimens with a compaction pressure of 35 MPa for a maximum strength of 63.1 N (decreased 11.37%) with a displacement of 6.8 mm.

The lowest bending strength was 55.7 N (21.76% decrease) with a displacement of 5.7 mm in the specimen for a compacting pressure of 30 MPa. Bending test results for specimens with higher pressure can increase mechanical strength and make the specimen stiffer. Research conducted by Haq. R et al. (2019), and Sadudeethanakul. S et al. (2019) is in line with this research. The bending strength of composite materials increases as the compaction of the material increases, thereby increasing the mechanical strength [28,64].

The concentration of nHA in the polymer matrix (PLA/PCL) with low compaction pressure resulted in nHA agglomeration. Consequently, propagation fractures can form as a result of stress concentration, decreasing the density value but increasing the displacement [65]. The compaction pressure is increased to be greater for the density to increase, the powder contact area is wider, the bending strength is increased, but the displacement is reduced and brittle [13,56,66].

Flexural strength increases as the dispersion of nHA particles increases, reducing porosity. Similar findings were reported by Nawang et al. (2019) an increase in the amount of nHA decreases the flexural strength even though the compaction pressure is increased [67]. Thus, the interfacial bond strength of the material and the flexural strength of the resulting composite material decrease [68]. The bending strength can be increased by adding higher compaction pressure [26]. However, the most optimal bending strength of this specimen is still below the bending strength of the femur of 130 N/mm^2 [25].

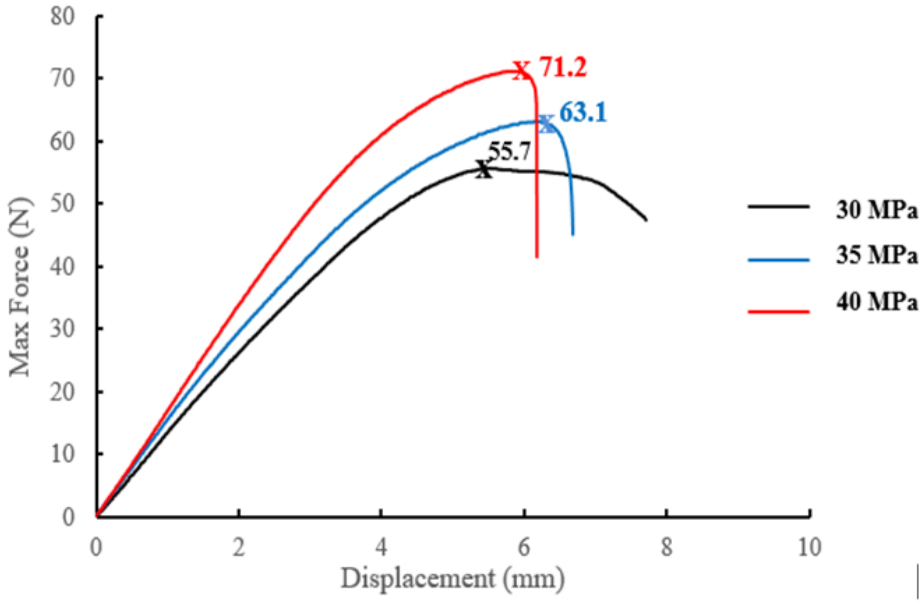

Figure 5. Bending test results for PLA/PCL/nHA composite materials

3.6. Tensile Test

Tensile testing on PLA/PCL/HA composite material specimens with compaction variations is shown in the stress-strain curve in Figure 6. Furthermore, from reading the stress-strain curve, the tensile strength (N/mm2) and elongation (mm) are obtained for each composite material specimen. PLA/PCL/nHA composite material specimens with a compaction pressure of 40 MPa had the highest tensile strength at 23.36 N/mm^2, yield strength of 21.88 N/mm^2 and strain of 3.62%. Compaction pressure was lowered to 35 MPa for tensile strength decreased by 4.88% (22.22 N/mm^2), yield strength was 20.66 N/mm^2 and elongation increased by 4.41%. The lowest tensile strength is 20.50 N/mm^2 with a yield strength of 18.65 N/mm^2 and an elongation of 4.53%.

The increase in compaction pressure greatly affects the PLA/PCL/nHA composite material in improving mechanical properties. This is in line with the tensile test results of the same specimen. These results prove that the greater the compaction pressure, the denser the material, the decreased porosity and increased tensile strength. The findings of this study are consistent with Xiong's. (2016) which found that high-density composites exhibited better mechanical properties [32]. However, the strain values of the three specimens of the PLA/PCL/nHA composite material were still low indicating their brittle nature. In the book Materials Science and Engineering an Introduction Tenth Edition states that a material is considered brittle if it has a strain of less than 5% [69]. Composite materials with a higher percentage of nHA can reduce the tensile strength and yield strength. This is because HA has high fragility and stiffness [37]. The nHA particles cause a longer fracture propagation path, absorb some of the energy, and increase plastic deformation, despite the high compaction pressure strength. In addition, the increased agglomeration of nHA particles resulting from uneven dispersion reduces the strength of the biocomposite [70,71].

The optimal tensile test results in the study were still below the tensile strength of the femur of 50 MPa, so it is necessary to add a higher compaction pressure [72].

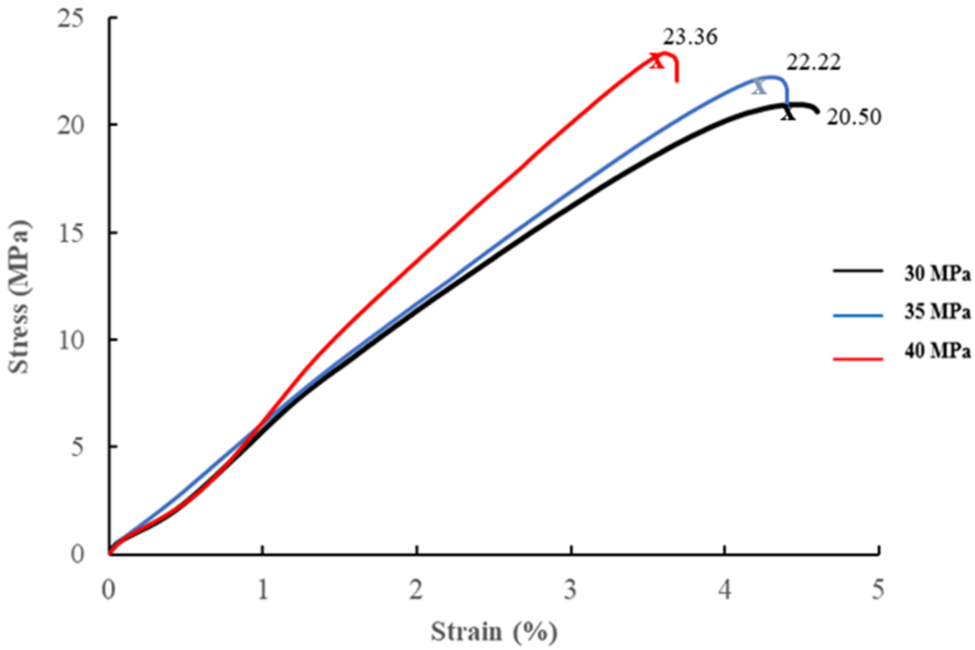

Figure 6. Tensile test results for PLA/PCL/nHA composite materials

4.0 Conclusions

The higher compaction pressure in the cold isostatic pressing method does not significantly affect the material properties, but can increase the mechanical strength of the specimen. This was proven by the FTIR test with the presence of identified band peaks from PLA, PCL, and nHA. This indicates the presence of a PLA/PCL/nHA composite material. The results of the XRD test for composite materials show a widened diffraction peak. This indicates the absence of crystal peaks in the composite material, proving an amorphous structure, low crystallinity, and faster degradation time. High compaction pressure reduces the size of the porosity, the surface is smoother, the interfacial bond is stronger and the density is higher.

The highest mechanical strength results were found in PLA/PCL/nHA composite materials at a compaction pressure of 40 MPa. The compressive strength results are 71.2 N and the tensile strength is 23.36 N/mm^2. The compressive and tensile strength in this study were still below the strength of the femur bone as an implant medium of 130 and 50 N/mm^2.

Acknowledgements

The author would like to thank Engeenering Faculty Universitas Muhammadiyah Semarang Indonesia, which has provided funding for Research disertation of fiscal year 2022-2023. The material characterization partially supported by research fund from Department Mechanical Engineering, Faculty of Engineering, Diponegoro University, 2023.

References

1. Desiartama, A., & Aryana, W. (2017). Gambaran Karakteristik Pasien Fraktur Femur Akibat Kecelakaan Lalu Lintas Pada Orang Dewasa Di Rumah Sakit Umum Pusat Sanglah Denpasar Tahun 2013. E-Jurnal Medika, 6(5), 1–4.
2. Wongchai, B. (2012). The effect of the configuration of the screw fixation on the interfragmentary strain. American Journal of Applied Sciences, 9(6), 842–845. https://doi.org/10.3844/ajassp.2012.842.845
3. Latif, M. N., Nabawi, R. A., Nanda, I. P., & Sahputra, R. E. (2019). Simulasi Dan Analisis Locking Compression Plate Implan Tulang Paha Menggunakan Metoda Finite Element Analysis. Jurnal Sains dan Teknologi, 19(1), 72–78.
4. Saidpour, S. H. (2006). Assessment of Carbon Fibre Composite Fracture Fixation Plate Using Finite Element Analysis. Annals of Biomedical Engineering, 34(7), 1157–1163. doi:10.1007/s10439-006-9102-z.
5. Ritonga, I. (2020). Karakteristik Implant Failure Pada Pasien Yang Menjalani Orif Plate And Screw Pada Anggota Gerak Bawah Di RSUP Ham Medan Tahun 2015-2019. Universitas Sumatera Utara Medan.
6. Juutilainen T, Pätiälä H, Ruuskanen M, Rokkanen P. Comparison of costs in ankle fractures treated with absorbable or metallic fixation devices. Arch Orthop Trauma Surg1997;116:204-8.
7. Böstman O., Pihlajamäki H., 1996, Routine implant removal after fracture surgery: a potentially reducible consumer of hospital resources in trauma units. J Trauma;41:846-9.
8. Rusrial, Gunawarman, & Affa, J. (2014). Pengaruh Ukuran serta Sudut Pemasangan Pin terhadap Kekuatan Sambungan Tulang Pasca Fraktur. 21(1), 55–59.
9. Triyono. J., 2015, Terinspirasi Kelainan Tulang, Suara Merdeka Cetak, www.berita.suaramerdeka.com, diakses pada tanggal Kamis , 2 April 2015.
10. Ciccone, W. J, Motz, C., Bentley, C., & Tasto, J. P. (2001). Bioabsorbable Implants in Orthopaedics: New Developments and Clinical Applications. The Journal of the American Academy of Orthopaedic Surgeons. https://doi.org/10.5435/00124635-200109000-00001
11. Toro C, Robiony M, Zerman N, Politi M., 2005, Resorbable plates in maxillary fixation. A 5year experience. Minerva Stomatol;54(4):199-206.

ISSN 2063-5346 *Section A-Research paper*

12. Solechan, Suprihanto, A., Widyanto, S. A., Triyono, J., Fitriyana, D. F., Siregar, J. P., & Cionita, T. (2022). Investigating the Effect of PCL Concentrations on the Characterization of PLA Polymeric Blends for Biomaterial Applications. Materials, 15. https://doi.org/https:// doi.org/10.3390/ma15207396 Academic

13. Böstman O., Pihlajamäki H, 2000, Clinical biocompatibility of biodegradable orthopaedic implants for internal fixation: a review. Biomaterials ;21:2615-21.

14. Vatchha, S. P., Kohli, A., Tripathi, S. K., & Nanda, S. N. (2015). Biodegradable Implants in Orthopaedics. Annals Of International Medical and Dental Reseach, 1(1), 3–8.

15. Golish SR., Mihalko WM., 2011, Principles of biomechanics and biomaterials in orthopaedic surgery. Instr Course Lect. 2011;60:575–581.

16. Dawoud. M., I. Taha, S.J. Ebeid., 2016, Mechanical behaviour of ABS: An experimental study using FDM and injection moulding techniques, Journal of Manufacturing Processes 21 39-45.

17. Lasprilla, A. J. R., Martinez, G. A. R., Lunelli, B. H., Jardini, A. L., & Maciel, R. (2012). Poly-lactic acid synthesis for application in biomedical devices — A review. Biotechnology Advances, 30, 321–328. https://doi.org/10.1016/j.biotechadv.2011.06.019

18. Pietrzykowska, E., Romelczyk-Baishya, B., Wojnarowicz, J., Sokolova, M., Szlazak, K., Swieszkowski, W.,Lojkowski, W., 2020, Preparation of a Ceramic Matrix Composite Made of Hydroxyapatite Nanoparticles and Polylactic Acid by Consolidation of Composite Granules. Nanomaterials, 10(6), 1060. doi:10.3390/nano10061060.

19. Matta, A. K., Rao, R. U., Suman, K. N. S., & Rambabu, V. (2014). Preparation and Characterization of Biodegradable PLA / PCL Polymeric Blends. Procedia Materials Science, 6(Icmpc), 1266–1270. https://doi.org/10.1016/j.mspro.2014.07.201

20. Mochane, M. J., Motsoeneng, T. S., Sadiku, E. R., Mokhena, T. C., & Sefadi, J. S. (2019). Morphology and properties of electrospun PCL and its composites for medical applications: A mini review. Applied Sciences (Switzerland), 9(11), 1–17. https://doi.org/10.3390/app9112205

21. Fong, M. K., Nasrull, M., Rahman, A., Mubarak, A., & Arifin, T. (2021). Characterization , Thermal and Biological Properties of PCL / PLA / PEG / N-HA Composites. 11(2), 9017–9026.

22. Neut, D., Kluin, O. S., Crielaard, B. J., Van Der Mei, H. C., Busscher, H. J., & Grijpma, D. W. (2009). A biodegradable antibiotic delivery system based on poly-(trimethylene carbonate) for the treatment of osteomyelitis. Acta Orthopaedica, 80(5), 514–519. https://doi.org/10.3109/17453670903350040

23. Malikmammadov, E., Tanir, T. E., Kiziltay, A., & Hasirci, V. (2018). PCL and PCL-Based Materials in Biomedical Applications PCL and PCL-based materials in biomedical applications. Journal of Biomaterials Science, Polymer Edition, 29, 863–893. https://doi.org/10.1080/09205063.2017.1394711

24. Ferri, J., M., Fenollar., O., Jorda-Vilaplana, A., García-Sanoguera, D., & Balart, R., 2016, Effect of miscibility on mechanical and thermal properties of poly(lactic acid)/ polycaprolactone blends. Polymer International, 65(4), 453–463. doi:10.1002/pi.5079.

25. P.Y.Chena, A.G.Stokesb, J. McKittrick, 2009, Comparison of the structure and mechanical properties of bovine femur bone and antler of the North American elk (Cervus elaphus canadensis), Acta

Biomaterialia, Volume 5, Issue 2, February 2009, Pages 693-706, https://doi.org/10.1016/j.actbio.2008.09.011

26. Fortelny, I., Ujcic, A., Fambri, L., & Slouf, M. (2019). Phase Structure , Compatibility , and Toughness of PLA / PCL Blends: A Review. 6, 1–13. https://doi.org/10.3389/fmats.2019.00206

27. Saifudin Alie Anwar., Solechan., 2015, studi pembuatan filamen komposit FDM untuk print 3D dari material Hidoryapatite bovine dan polimer PCL untuk scaffolds mandibular, Jurnal Gardan, vol 2 edisi 1, hal 6-12.

28. Sadudeethanakul, S., Wattanutchariya, W., Nakkiew, W., Chaijaruwanich, A., & Pitjamit, S. (2019). Bending strength and Biological properties of PLA- HA composites for femoral canine bone fixation plate. IOP Conference Series: Materials Science and Engineering. https://doi.org/10.1088/1757-899X/635/1/012004

29. Cardoso, G.B.C.; Ramos, S.L.F.; Rodas, A.C.D.; Higa, O.Z.; Zavaglia, C.A.C.; Arruda, A.C.F. Scaffolds of Poly (ε-Caprolactone) with Whiskers of Hydroxyapatite. J. Mater. Sci. 2010, 45, 4990–4993, doi:10.1007/s10853-010-4363-1.

30. Ali, J., Rezaei-tavirani, M., Biazar, E., K, S. H., & Jahandideh, R. (2011). Mechanical Properties of Chitosan-Starch Composite Filled Hydroxyapatite Micro- and Nanopowders. Hindawi Publishing Corporation Journal of Nanomaterials, 2011, 18–23. https://doi.org/10.1155/2011/391596

31. Alizadeh-osgouei, M., Li, Y., & Wen, C. (2019). A comprehensive review of biodegradable synthetic polymer-ceramic composites and their manufacture for biomedical applications. Bioactive Materials, 4(1), 22–36. https://doi.org/10.1016/j.bioactmat.2018.11.003

32. Xiong, G., Nie, Y., Ji, D., Li, J., Li, C., Li, W., Zhu, Y., Luo, H., & Wan, Y. (2016). Characterization of biomedical hydroxyapatite/magnesium composites prepared by powder metallurgy assisted with microwave sintering. Current Applied Physics, 8, 830–836. https://doi.org/http://dx.doi.org/10.1016/j.cap.2016.05.004

33. Cóta, L. F., Patricia, K., Licona, M., Lunz, N., Ribeiro, A. A., Morejón, L., Oliveira, M. V. De, & Pereira, L. C. (2016). Hydroxyapatite Nanoparticles: Synthesis by Sonochemical Method and Assessment of Processing Parameters via Experimental Design. Materials Science Forum, 869, 896–901. https://doi.org/10.4028/www.scientific.net/MSF.869.896

34. Morris, K.J. 1991, Cold Isostatic Pressing. In Concise Encyclopedia of Advanced Ceramic Materials; BROOK, R.J.B.T.-C.E. of A.C.M., Ed.; Pergamon: Oxford, 1991; pp. 84–88 ISBN 978-0-08-034720-2.

35. German RM, Bose A., 1997, Injection Molding of Metals and Ceramics: Metal Powder Industries Federation. ISBN 187895461X, 9781878954619

36. Arifin, A., Sulong, A. B., Muhamad, N., Syarif, J., & Ramli, M. I. 2014, Material processing of hydroxyapatite and titanium alloy (HA/Ti) composite as implant materials using powder metallurgy: A review. Materials & Design, 55, 165–175. doi:10.1016/j.matdes..09.045

37. Solechan, Prasetyo, M. T., Triyono, J., & Pujiyanto, E. (2021). Pengujian Sifat Mekanik Implan Plate dan Sekrup Fiksasi Internal Tulang Femur Dari Material Hidroksiapatit Bovine Dan Polimer Biodegradasi Menggunakan Printer 3D. TRAKSI: Majalah Ilmiah Teknik Mesin, 20(1), 45–58. https://doi.org/https://dx.doi.org/10.26714/traksi.21.1.2021.27-37

38. Fitriyana, D.F.; Nugraha, F.W.; Laroybafih, M.B.; Ismail, R.; Bayuseno, A.P.; Muhamadin, R.C.; Ramadan, M.B.; Qudus, A.R.A.; Siregar, J.P. The Effect of Hydroxyapatite Concentration on the Mechanical Properties and Degradation Rate of Biocomposite for Biomedical Applications. IOP Conf. Ser. Earth Environ. Sci. 2022, 969, 12045, doi:10.1088/1755-1315/969/1/012045.

39. Balbinotti P., Gemelli E., Buerger G., de Lima SA., de Jesus J., Camargo NHA., et al, 2011, Microstructure Development on Sintered Ti/HA Biocomposites Produced by Powder Metallurgy. Mater Res-Ibero-Am J. ;14:384-93.

40. Guangyao Xiong., Yanjiao Nie., Dehui Ji, Jing Li., Chunzhi Li., Wei Li., Yong Zhu., Honglin Luo., Yizao Wan., 2016. Characterization of biomedical hydroxyapatite/magnesium composites prepared by powder metallurgy assisted with microwave sintering. Current Applied Physics, 16(8), 830–836. doi:10.1016/j.cap.2016.05.004

41. Hassanajilia. H, Ali Karami-Poura, Ahmad Oryanb, Tahereh Talaei-Khozanic, 2019, Preparation and characterization of PLA/PCL/HA composite scaffolds using indirect 3D printing for bone tissue engineering, Materials Science & Engineering C 104. 109960, https://doi.org/10.1016/j.msec.2019.109960

42. Singla, P., Mehta, R., Berek, D., & Upadhyay, S. N. (2012). Microwave Assisted Synthesis of Poly (Lactic acid) and its Characterization using Journal of Macromolecular Science , Part A : Pure and Applied Chemistry Microwave Assisted Synthesis of Poly (lactic acid) and its Characterization using Size Exclusion. Journal of Macromolecular Science, Part A: Pure and Applied Chemistry, 49(11), 963–970. https://doi.org/10.1080/10601325.2012.722858

43. Prajongtat, P., Sriprachuabwong, C., Wongkanya, R., & Dechtrirat, D. (2019). Moisture-Resistant Electrospun Polymer Membranes for Efficient and Stable Fully Printable Perovskite Solar Cells Prepared in Humid Air Moisture-Resistant Electrospun Polymer Membranes for E ffi cient and Stable Fully Printable Perovskite Solar Cells Prepa. August. https://doi.org/10.1021/acsami.9b05032

44. Rasal, R. M., Janorkar, A. V, & Hirt, D. E. (2010). Progress in Polymer Science Poly (lactic acid) modifications. Progress in Polymer Science, 35(3), 338–356. https://doi.org/10.1016/j.progpolymsci.2009.12.003

45. Dahlan, K., Sari, Y. W., Yuniarti, E., & Soejoko, D. S. (2006). Karakterisasi Gugus Fosfat dan Karbonat dalam Tulang Tikus dengan Fourier Transform Infrared (FT-IR) Spectroscopy. Indonesian Journal of Materials Science, 221–224.

46. Lu, Y., Chen, Y., & Zhang, P. (2016). Preparation and Characterisation of Polylactic Acid (PLA)/ Polycaprolactone (PCL) Composite Microfibre Membranes. FIBRES & TEXTILES in Eastern Europe, 24(117), 17–25. https://doi.org/10.5604/12303666.1196607

47. Hooshmand, T., Abrishamchian, A., Najafi, F., Mohammadi, M., Najafi, H., & Tahriri, M. (2014). Development of sol-gel-derived multi-wall carbon nanotube / hydroxyapatite nanocomposite powders for bone substitution. Journal of Composite Materials 0(0), 1–7. https://doi.org/10.1177/0021998313475368

48. Hou, A.-L., & Qu, J.-P. (2019). Super-Toughened Poly(lactic Acid) with Poly(ε-caprolactone) and Ethylene-Methyl Acrylate-Glycidyl Methacrylate by Reactive Melt Blending Ao-Lin. Polymers.

ISSN 2063-5346 *Section A-Research paper*

49. Silverajah, V.S.G.; Ibrahim, N.A.; Yunus, W.M.Z.W.; Hassan, H.A.; Woei, C.B. A Comparative Study on the Mechanical, Thermal and Morphological Characterization of Poly(Lactic Acid)/Epoxidized Palm Oil Blend. Int. J. Mol. Sci. 2012, 13, 5878–5898.

50. Hasan, A.; Soliman, S.; El Hajj, F.; Tseng, Y.T.; Yalcin, H.C.; Marei, H.E. Fabrication and in Vitro Characterization of a Tissue Engineered PCL-PLLA Heart Valve. Sci. Rep. 2018, 8, 1–14, doi:10.1038/s41598-018-26452-y.

51. Jing, X.; Mi, H.-Y.; Turng, L.-S. Comparison between PCL/Hydroxyapatite (HA) and PCL/Halloysite Nanotube (HNT) Composite Scaffolds Prepared by Co-Extrusion and Gas Foaming. Mater. Sci. Eng. C 2017, 72, 53–61, doi:https://doi.org/10.1016/j.msec.2016.11.049.

52. Gong, M., Zhao, Q., Dai, L., Li, Y., & Jiang, T. (2017). Journal of Asian Ceramic Societies Fabrication of polylactic acid / hydroxyapatite / graphene oxide composite and their thermal stability , hydrophobic and mechanical properties. Integrative Medicine Research, 5(2), 160–168. https://doi.org/10.1016/j.jascer.2017.04.001

53. Pitjamit, S.; Thunsiri, K.; Nakkiew, W.; Wongwichai, T. The Possibility of Interlocking Nail Fabrication from FFF 3D Printing PLA/PCL/HA Composites Coated by Local Silk Fibroin for Canine Bone Fracture Treatment. Materials (Basel). 2020, 13.

54. Doyle, S.E.; Henry, L.; McGennisken, E.; Onofrillo, C.; Di Bella, C.; Duchi, S.; O'connell, C.D.; Pirogova, E. Characterization of Polycaprolactone Nanohydroxyapatite Composites with Tunable Degradability Suitable for Indirect Printing. Polymers (Basel). 2021, 13, 1–14, doi:10.3390/polym13020295.

55. Satapathy, B.P.N. and A. Processing and Characterization of Epoxy Composites Reinforced with Short Human Hair. J. Phys. Conf. Ser. 2017, 178, 1–7, doi:10.1088/1742-6596/755/1/011001.

56. Groover MP., 2010, Fundamentals of Modern Manufacturing: Materials 4th edition, Processes, and Systems: John Wiley & Sons; Professor of Industrial and Systems Engineering Lehigh University

57. Triyono, J., Alfiansyah, R., Sukanto, H., Ariawan, D., & Nugroho, Y. (2020). Fabrication and characterization of porous bone scaffold of bovine hydroxyapatite-glycerin by 3D printing technology. Bioprinting, e00078. doi:10.1016/j.bprint.2020.e00078

58. Molinero-Mourelle, P.; Canals, S.; Gómez-Polo, M.; Sola-Ruiz, M.; Highsmith, J.D.R.; Viñuela, A. Polylactic Acid as a Mate-rial for Three-Dimensional Printing of Provisional Restorations. Int. J. Prosthodont. 2018, 31, 349–350. https://doi.org/10.11607/ijp.5709.

59. Leno, M. B., Liu, S. Y., Chen, C. T., & Liao, H. T, 2017, Comparison of functional outcomes and patient-reported satisfaction between titanium and absorbable plates and screws for fixation of mandibular fractures: A one-year prospective stu.

60. Randall M. German and Animesh Bose, 2020, Binder and Polymer Assisted Powder Processing, Publisher: ASM International, Pages: 273, ISBN: 978-1-62708-275-4, Product code: 05929G.

61. Abbasi, N.; Hamlet, S.; Love, R.M.; Nguyen, N.-T. Porous Scaffolds for Bone Regeneration. J. Sci. Adv. Mater. Devices 2020, 5, 1–9, doi:https://doi.org/10.1016/j.jsamd.2020.01.007.

62. Åkerlund, E.; Diez-escudero, A.; Grzeszczak, A. The Effect of PCL Addition on 3D-Printable PLA / HA Composite Filaments for the Treatment of Bone Defects. Polymers (Basel). 2022, 14, 1–17.

63. Fang, Z.; Feng, Q. Improved Mechanical Properties of Hydroxyapatite Whisker-Reinforced Poly(l-Lactic Acid) Scaffold by Surface Modification of Hydroxyapatite. Mater. Sci. Eng. C 2014, 35, 190–194, doi:10.1016/j.msec.2013.11.008.
64. Haq, R., Haq, A., Taib, I., Nasrull, M., Rahman, A., Haw, F., Abdullah, H., Ahmad, S., Mubarak, A., Ariffin, T., & Hassan, M. F. (2019). Mechanical Properties of PCL / PLA Composite Sample Produced from 3D Printer and Injection Molding. 5, 97–101.
65. Aldabib, J.M.; Ishak, Z.A.M. Effect of Hydroxyapatite Filler Concentration on Mechanical Properties of Poly (Methyl Methacrylate) Denture Base. SN Appl. Sci. 2020, 2, 1–14, doi:10.1007/s42452-020-2546-1.
66. Qureshi, Z.A., Salah Addin Burhan Al-Omaria, Emad Elnajjara Oraib, Al-Ketanb Rashid Abu Al-Rubc., 2022., On the effect of porosity and functional grading of 3D printable triply periodic minimal surface (TPMS) based architected lattices embedded with a phase change material., International Journal of Heat and Mass Transfer., Volume 183, https://doi.org/10.1016/j.ijheatmasstransfer.2021.122111.
67. Nawang, R.; Hussein, M.Z.; Matori, K.A.; Che Abdullah, C.A.; Hashim, M. (2019). Physicochemical Properties of Hydroxyapatite/Montmorillonite Nanocomposite Prepared by Powder Sintering. Results Phys. 2019, 15, 102540, doi:https://doi.org/10.1016/j.rinp.2019.102540.
68. Hapsari, D.N.; Wardani, S.C.; Firdausya, W.A.; Amaturrohman, K.; Wiratama, H.P. The Effect of Addition of Hydroxyapatite from Skipjack Tuna (Katsuwonus Pelamis) Fish Bone Flour to the Transverse, Impact, and Tensile Strength of Heat Cured Acrylic Resin. J. Dentomaxillofacial Sci. 2020, 5, 94, doi:10.15562/jdmfs.v5i2.1016.
69. Callister, W. D., & Rethwisch, D. G. (2018). Materials Science and Engineering An Introduction Tenth Edition (10th Edition). Department of Metallurgical Engineering. The University of Utah and The University of Iowa. John Wiley & Sons, Inc.
70. Dehestani, M.; Adolfsson, E.; Stanciu, L.A. Mechanical Properties and Corrosion Behavior of Powder Metallurgy Iron-Hydroxyapatite Composites for Biodegradable Implant Applications. Mater. Des. 2016, 109, 556–569, doi:10.1016/j.matdes.2016.07.092.
71. Kang, J.; Zheng, J.; Hui, Y.; Li, D. Mechanical Properties of 3D-Printed PEEK/HA Composite Filaments. Polymers (Basel). 2022, 14, doi:10.3390/polym14204293.
72. Corcione, C.E., F. Gervaso., F. Scalera., F. Montagna., T. Maiullaro., A. Sannino., A. Maffezzoli., 2017, 3D printing of hydroxyapatite polymer-based composites for bone tissue engineering, J. Polym. Eng 741.